


## Article

# Variations and Trends in 115 Years of Graded Daily Precipitation Records at Three Hydrometeorological Stations in Finland

Masoud Irannezhad <sup>1,2,\*</sup> , Zahrah Abdulghafour <sup>1</sup>, Retaj AlQallaf <sup>1</sup>, Fadak Abdulreda <sup>1</sup>, Ghadeer Shamsah <sup>1</sup> and Hajar Alshammari <sup>1</sup>

<sup>1</sup> Department of Civil Engineering, College of Engineering, Australian University, West Mishref, Safat 13015, Kuwait; zahrah.abdulghafour@gmail.com (Z.A.); ritajalqallaf@outlook.com (R.A.); fadak17@outlook.com (F.A.); gs22x.s@gmail.com (G.S.); alshmmeryhajar@gmail.com (H.A.)

<sup>2</sup> Water, Energy and Environmental Engineering Research Unit, Faculty of Technology, University of Oulu, 90014 Oulu, Finland

\* Correspondence: m.irannezhad@au.edu.kw; Tel.: +965-66102526

**Abstract:** This study investigated the variability and trends in 115 years (1909–2023) of daily precipitation observed at three hydrometeorological stations in southern (Kaisaniemi), central (Kajaani), and northern (Sodankylä) Finland. We also identified the most significant climate teleconnections influencing daily precipitation variability at these three stations during the period 1951–2023. The daily precipitation records were primarily classified into six grades, including very light ( $\leq 1$  mm), light ( $1 < \leq 5$  mm), moderate ( $5 < \leq 10$  mm), heavy ( $10 < \leq 15$  mm), very heavy ( $15 < \leq 20$  mm), and extreme ( $> 20$  mm). On average, the most intense daily precipitation was determined at the Kaisaniemi station in southern Finland. At this station, however, very light and light precipitation showed the lowest frequency, but other graded daily precipitation events were the most frequent. At all three stations, the intensity of very light precipitation significantly declined during the past 115 years, while its frequency increased. The highest rates of such decreases and increases in the intensity and frequency of very light daily precipitation were found at the Sodankylä stations in northern Finland, respectively, but the lowest rates were at the Kaisaniemi station in the south. At the Kajaani station in central Finland, the intensity of light precipitation decreased, but very heavy precipitation intensified. At this station, however, the number of both moderate and heavy precipitation events increased over time. Finally, historical variations in both the intensity and frequency of graded daily precipitation events in Finland showed significant relationships with different climate teleconnections, particularly the Scandinavia (SCAND) and the North Atlantic Oscillation (NAO) patterns.

**Keywords:** frequency; intensity; precipitation; teleconnections; trend; water resources



**Citation:** Irannezhad, M.; Abdulghafour, Z.; AlQallaf, R.; Abdulreda, F.; Shamsah, G.; Alshammari, H. Variations and Trends in 115 Years of Graded Daily Precipitation Records at Three Hydrometeorological Stations in Finland. *Water* **2024**, *16*, 2684. <https://doi.org/10.3390/w16182684>

Academic Editor: Paul Kucera

Received: 23 August 2024

Revised: 17 September 2024

Accepted: 18 September 2024

Published: 20 September 2024



**Copyright:** © 2024 by the authors. Licensee MDPI, Basel, Switzerland. This article is an open access article distributed under the terms and conditions of the Creative Commons Attribution (CC BY) license (<https://creativecommons.org/licenses/by/4.0/>).

## 1. Introduction

Global mean surface air temperature (SAT) warmed by 1.09 °C in 2011–2020, compared to the period 1850–1900, particularly in response to the significant increases in the anthropogenic concentrations of greenhouse gas (GHG) emissions to the Earth's atmosphere [1]. Sea surface temperature (SST) also increased worldwide, mainly due to the significantly higher atmospheric CO<sub>2</sub> concentration in recent decades [2]. Based on the Clausius–Clapeyron (C–C) relationship, such warmer SAT and SST fundamentally increase atmospheric moisture content [3], thereby particularly leading to significant changes in different characteristics (mainly in terms of intensity and frequency) of extreme precipitation events (EPEs) around the world [4–6]. Such alterations in EPEs have already posed serious economic, social, and environmental sustainability challenges to humanity, particularly in developing countries with high population density, vulnerable infrastructures, and poor land-use management [7].

Globally, the intensity and frequency of EPEs have substantially increased in recent decades [1]. However, these increases are not essentially translated to similar alterations in

such characteristics of EPEs on regional and local scales [8]. To investigate historical and future changes in EPEs around the world, most of the previous studies [9–11] applied a set of extreme precipitation indices recommended by the Expert Team on Climate Change Detection and Indices (ETCCDI) [12]. These extreme indices were principally developed based on daily precipitation amounts less, equal to, or greater than a couple of predefined absolute values, threshold numbers, or long-term  $NN^{\text{th}}$  percentiles (e.g.,  $NN = 99$ ) [13]. There are also several studies [14–16] focusing on extreme value analysis (EVA) approaches, like the peak-over-threshold (POT), for evaluating spatio-temporal variability and changes in regional and local EPEs. A few other studies, however, defined the characteristics of EPEs based on different grades of daily precipitation amounts [17–19]. Although we have already applied extreme precipitation indices [20] and the POT approach [21] for investigating spatio-temporal changes in EPEs in Finland, there is still a lack of studies on variations and trends in graded daily precipitation records throughout this country.

In the era of global warming, it is not only important to investigate regional precipitation changes but also to explain their different underlying physical mechanisms. In hydrology, the spatio-temporal variability across a region is generally related to the atmospheric water content sources and transport paths [22] naturally controlled by different large-scale patterns in atmospheric circulation around the Earth [23–25]. In general, these patterns refer to stable, repeating, and extensive modes of atmospheric pressure anomalies exposing the predominant airflow across a widespread geographical area [26]. They also describe the persistent variability in the natural incidence of chaotic actions in the global climate system [27]. The strength and effects of such patterns across a region through a certain period of the year are principally quantified by numerical indices called “climate teleconnections” [27]. The primary components of such climate teleconnections and their effects on historical variability in regional EPEs around the world have been previously reviewed [6,28–32]. For Finland, we already reported influential climate teleconnections for variability in EPEs identified by applying the extreme precipitation indices [20] and the POT approach [21]. However, understanding and explaining the role of climate teleconnections in the spatio-temporal variability and trends in historically graded daily precipitation records throughout Finland is still well motivated.

This study aimed to investigate long-term historical graded daily precipitation events throughout Finland and their relationships with the well-known large-scale climate teleconnections. Accordingly, the specific objectives were to: (1) summarize statistical analyses of 115-year (1909–2023) graded daily precipitation records at three hydrometeorological stations in northern, central, and southern Finland; (2) determine significant trends in both the intensity and frequency of such historical graded daily precipitation records; and (3) identify influential climate teleconnections strongly influencing such variabilities and trends in historical graded daily precipitation events throughout the country. Based on [33], such observational studies can improve our knowledge about the effects of global warming on climatic conditions and, consequently, water resources availability in cold regions, playing an important role in acting towards achieving the 2030 United Nations Sustainable Development Goals (SDGs) adopted in 2015 [34].

## 2. Materials and Methods

### 2.1. Study Area and Data Used

Finland is located in the boreal environment [35] of northern Europe (Figure 1a). Its climate is substantially affected by the latitudinal gradient, the Baltic Sea, the Scandinavian mountains, the Atlantic Ocean, and continental Eurasia [36]. Based on the Köppen–Geiger climate classification system, Finland generally experiences no dry season [37]. In this country, summers are warm and mild (Dfb) in southwestern coastal areas while cold and short (Dfc) in most other parts [37]. However, a strong latitudinal gradient significantly controls SAT variability in Finland. Accordingly, both annual mean SAT [38] and precipitation [39] naturally increase in the south to north direction throughout this country (Figure 1b,c).

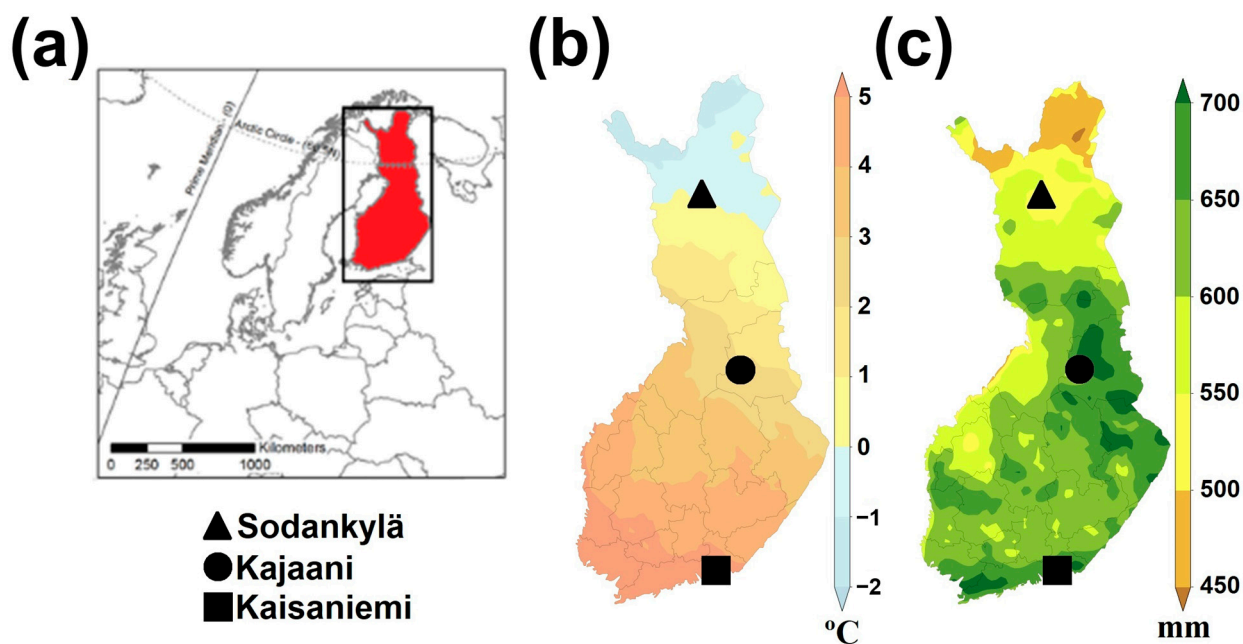


**Figure 1.** Map of (a) northern Europe with Finland colored red; (b) average of annual mean SAT (°C) and (c) average of annual precipitation (mm) throughout Finland during the latest normal climate period (1991–2020). Assembled based on [40].

For this study, three hydrometeorological stations of Kaisaniemi, Kajaani, and Sodankylä in southern, central, and northern Finland, respectively, were selected (Figure 1). These stations (i) have 115 years of daily precipitation records from 1909 to 2023; (ii) represent all three southern, central, and northern latitudes of Finland; and (iii) show the spatial pattern of precipitation distribution throughout the country. In our previous studies [41–43], we comprehensively explained the geographical coordinates, climatic conditions, devices, and techniques for measuring precipitation at all three Kaisaniemi, Kajaani, and Sodankylä stations. During the 115 years, a few hundred meters of dislocation of the stations, a minor missing data percentage, and a small difference in summertime precipitation due to applying different measuring devices and techniques were almost inevitable [44]; however, it might not practically influence long-term precipitation variability and trend analyses [42].

According to our current knowledge about the large-scale atmospheric circulation patterns influencing SAT and precipitation patterns in Finland [38,39,45,46], this study selected six climate teleconnections (Nos. 1–6 in Table 1). The main features and mechanisms of such teleconnections, as well as their natural influences on climate variability across northern Europe, are completely explained by [27]. Based on the 1981–2010 climatology, the standardized monthly time series (since January 1950) of these six climate teleconnections were obtained from the Climate Prediction Center (CPC) at the National Oceanic and Atmospheric Administration (NOAA), USA, freely available at <https://www.cpc.ncep.noaa.gov/data/teledoc/telecontents.shtml> (accessed on 10 January 2024). For this study, the average values of these monthly time series from January to December during a year were calculated as annual climate teleconnections for the years 1950–2023. Using the standardized monthly time series, seasonal climate teleconnections for winter (December–February), spring (March–May), summer (June–August), and autumn (September–November) for the years 1951–2023 were also calculated. Accordingly, for example, winter 1951 (2023) referred to the period between 1 December 1950 (2022) and the end of February 1951 (2023).

**Table 1.** Summary of climate teleconnections considered for this study.

No.	ID	Climate Teleconnection	Source	References
1	AO	Arctic Oscillation	CPC	[47]
2	EA	East Atlantic	CPC	[48]
3	EA/WR	East Atlantic/West Russia	CPC	[48,49]
4	NAO	North Atlantic Oscillation	CPC	[48]
5	POL	Polar/Eurasia pattern	CPC	[48]
6	SCAND	Scandinavia pattern	CPC	[48,50]

### 2.2. Intensity and Frequency Indices

A number of intensity and frequency indices were defined to analyze historical daily precipitation characteristics in Finland based on 1, 5, 10, 15, and 20 mm boundaries [17], grouped into two categories: long-term (Table 2) and annual (Table 3). The long-term intensity indices were used to investigate statistical characteristics of graded daily precipitation records during the full 115 years of our study period (1909–2023). However, the annual indices were employed for determining statistically significant trends in interannual fluctuations of graded daily precipitation intensity and frequency during the period 1909–2023. Similarly, the long-term frequency indices were also described by their interannual variations.

**Table 2.** Long-term intensity and frequency indices used to analyze historical daily precipitation in Finland based on 1, 5, 10, 15, and 20 mm boundaries.

Characteristic	ID	Description	Units
Intensity	iVLPt	0 mm < Daily precipitation ≤ 1 mm	mm day <sup>-1</sup>
	iLPt	1 mm < Daily precipitation ≤ 5 mm	
	iMPt	5 mm < Daily precipitation ≤ 10 mm	
	iHPt	10 mm < Daily precipitation ≤ 15 mm	
	iVHPt	15 mm < Daily precipitation ≤ 20 mm	
	iEPt	Daily precipitation ≥ 20 mm	
Frequency	fVLPt	0 mm < Number of daily precipitation events ≤ 1 mm	days year <sup>-1</sup>
	fLPt	1 mm < Number of daily precipitation events ≤ 5 mm	
	fMPt	5 mm < Number of daily precipitation events ≤ 10 mm	
	fHPt	10 mm < Number of daily precipitation events ≤ 15 mm	
	fVHPt	15 mm < Number of daily precipitation events ≤ 20 mm	
	fEPt	Number of daily precipitation events ≥ 20 mm	

Note: i: intensity; V: very; L: light; M: moderate; H: heavy; E: extreme; Pt: daily precipitation; and f: frequency.

### 2.3. Statistical Analyses

The Mann-Kendall non-parametric test was [51,52] applied for detecting statistically significant ( $p < 0.05$ ) trends in annual intensity and frequency indices at all stations studied during the period 1909–2023. However, the trend-free pre-whitening (TFPW) method [53] was used to determine statistically significant ( $p < 0.05$ ) trends in time series for annual intensity and frequency indices with positive autocorrelation. To calculate the magnitude of such significant trends, the Sen’s slope method [54] was employed. The slope of trends in annual intensity and frequency indices were normalized by their long-term (1909–2023) median values, expressed as a percentage. The Spearman’s rank correlation ( $\rho$ ) [55] was used to measure relationships of annual intensity and frequency indices with different climate teleconnections during the period 1951–2023. In the existence of autocorrelation in the time series studied, the residual bootstrap (RB) method [56] with 5000 independent replications was applied for estimating the standard deviations of the  $|\rho$ -values. Such statistical approaches have commonly been used in previous studies investigating climate change and its impacts on hydrology and water resources around the world [57–61].

**Table 3.** Annual intensity and frequency indices used to analyze historical daily precipitation in Finland based on 1, 5, 10, 15, and 20 mm boundaries.

Characteristic	ID	Description	Units
Intensity	iAAVLPt	Ratio of annual total precipitation for (0 mm < daily precipitation ≤ 1 mm) to number of occurrences for each year	mm day <sup>-1</sup> year <sup>-1</sup>
	iAALPt	Ratio of annual total precipitation for (1 mm < daily precipitation ≤ 5 mm) to number of occurrences for each year	
	iAAMPt	Ratio of annual total precipitation for (5 mm < daily precipitation ≤ 10 mm) to number of occurrences for each year	
	iAAHPt	Ratio of annual total precipitation for (10 mm < daily precipitation ≤ 15 mm) to number of occurrences for each year	
	iAAVHPt	Ratio of annual total precipitation for (15 mm < daily precipitation ≤ 20 mm) to number of occurrences for each year	
	iAAEPt	Ratio of annual total precipitation for (daily precipitation ≥ 20 mm) to number of occurrences for each year	
Frequency	fACVLPt	Number of events (0 mm < daily precipitation ≤ 1 mm) for each year	days year <sup>-1</sup>
	fACLPEt	Number of events (1 mm < daily precipitation ≤ 5 mm) for each year	
	fACMPt	Number of events (5 mm < daily precipitation ≤ 10 mm) for each year	
	fACHPEt	Number of events (10 mm < daily precipitation ≤ 15 mm) for each year	
	fACVHPt	Number of events (15 mm < daily precipitation ≤ 20 mm) for each year	
	fACEPEt	Number of days with precipitation ≥ 20 mm	

Note: i: intensity; AA: average annual; V: very; L: light; M: moderate; H: heavy; E: extreme; Pt: daily precipitation; P: Precipitation; f: frequency; AC: annual count; and Et: events.

### 3. Results

On average, the amount of very light daily precipitation (iVLPt) in Finland during the period 1909–2023 ranged from 0.31 to 0.44 mm (Figure 2a). Such graded daily precipitation events were mostly measured in 53–130 days of a year (Figure 2e). Interestingly, the Sodankylä station experienced the lowest intensity (Figure 2a) but the highest frequency (Figure 2e) of very light daily precipitation events. The light daily precipitation (iLPt) was between 2.35 and 2.73 mm (Figure 2b), observed in 55–93 days per year (Figure 2f). The most intense (iLPt) (Figure 2b) and frequent (fLPt) (Figure 2f) light daily precipitation events were usually experienced at the Kajaani station in central Finland. The highest intensities (iMPt, iHPt, iVHPt, and iEPt) and frequencies (fMPt, fHPt, fVHPt, and fEPt) of daily precipitation greater than 5 mm were generally recorded at the Kaisaniemi station in southern Finland (Figure 2b–d,f–h). The range of moderate daily precipitation intensity (iMPt) was from 6.70 to 7.30 mm (Figure 2b), occurring 32–37 times per year (Figure 2f). In Finland, both the intensities (Figure 2c,d) and frequencies (Figure 2g,h) of all heavy, very heavy, and extreme daily precipitation events increased from the north (Sodankylä) to south (Kaisaniemi) direction. The only exception referred to the lower frequency of extreme daily precipitation (fEPt) in central (Kajaani) rather than in northern (Sodankylä) Finland (Figure 2h). The intensity of extreme daily precipitation events (Figure 2d) ranged between 22.10 and 33.34 mm, experienced only 1–8 times in each year (Figure 2h).

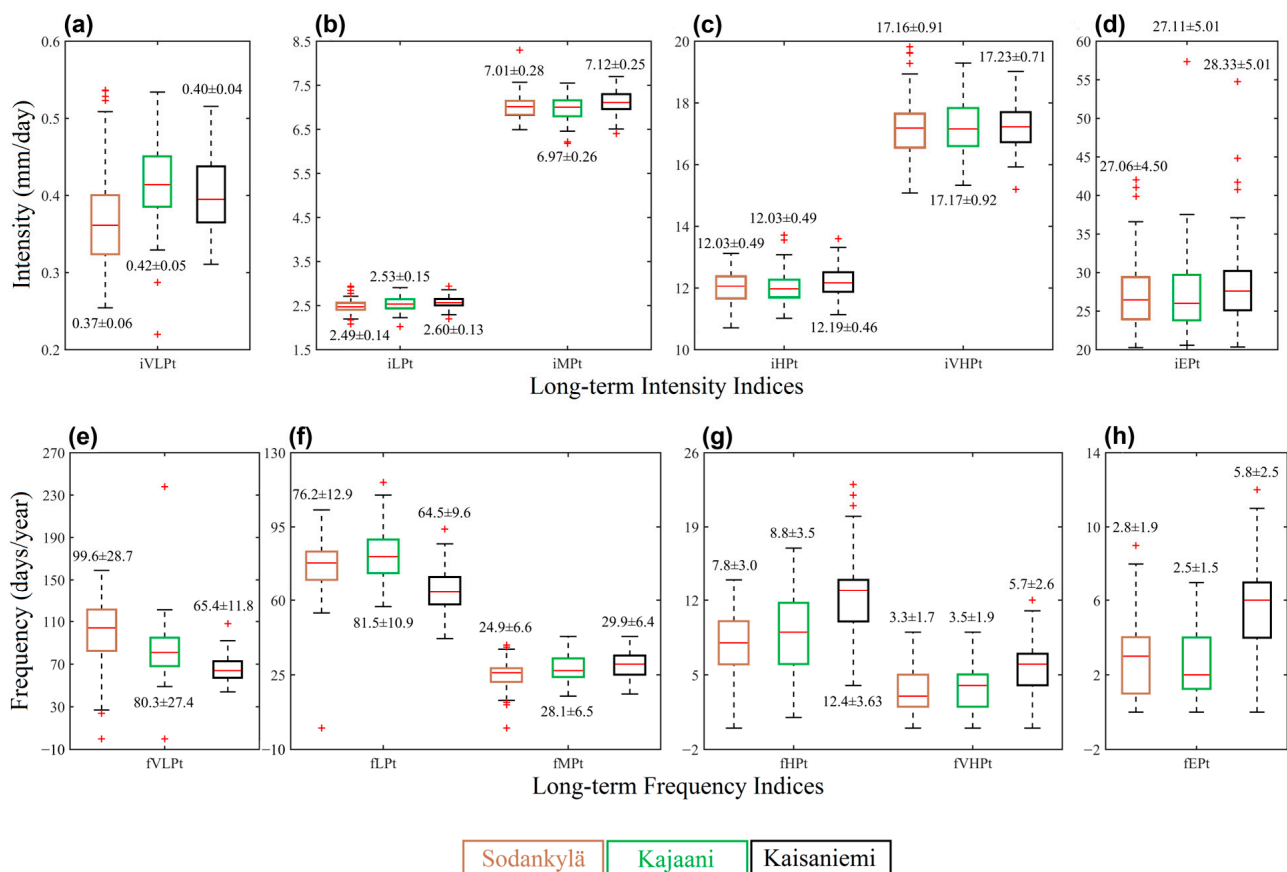


**Figure 2.** Box-and-whisker plots of long-term (1909–2023) daily precipitation (a–d) intensity and (e–h) frequency indices (Table 2) at the Sodankylä, Kajaani, and Kaisaniemi stations in northern, central, and southern Finland, respectively. Mean value ( $\mu$ )  $\pm$  standard deviation ( $\sigma$ ) as statistical parameters are given on top of each index. The outliers are represented by red “+” symbols.

The annual average intensity of very light daily precipitation events (iAAVLPt) showed statistically significant ( $p < 0.05$ ) decreasing trends, ranging from 0.36 to 0.42%, at all three stations studied during the period 1909–2023 (Figure 3a). However, the annual frequency of such events (iACVLPt) substantially increased by 64% at Sodankylä, 81% at Kajaani, and 104% at Kaisaniemi (Figure 3b). At Kajaani in central Finland, the annual intensity of light daily precipitation (iAALPt) decreased by 2.54%, while there was an increasing trend (by 17.16%) in the annual intensity of very high daily precipitation time series (Figure 3a). At this station (Kajaani), significant trends were found in the annual frequencies of both moderate (fACMPt) and high (fACHPt) daily precipitation events at the rates of 27% and 9%, respectively (Figure 3b). The Kaisaniemi station experienced substantial decreasing trends in the annual intensity of moderate daily precipitation (iAAMPt) and the annual frequency of extreme precipitation events (fACEPt) during the 100-years study period (Figure 3b). At Sodankylä in northern Finland, no significant trends were found in annual intensity and frequency indices other than iAAVLPt and FACVLPt (Figure 3).

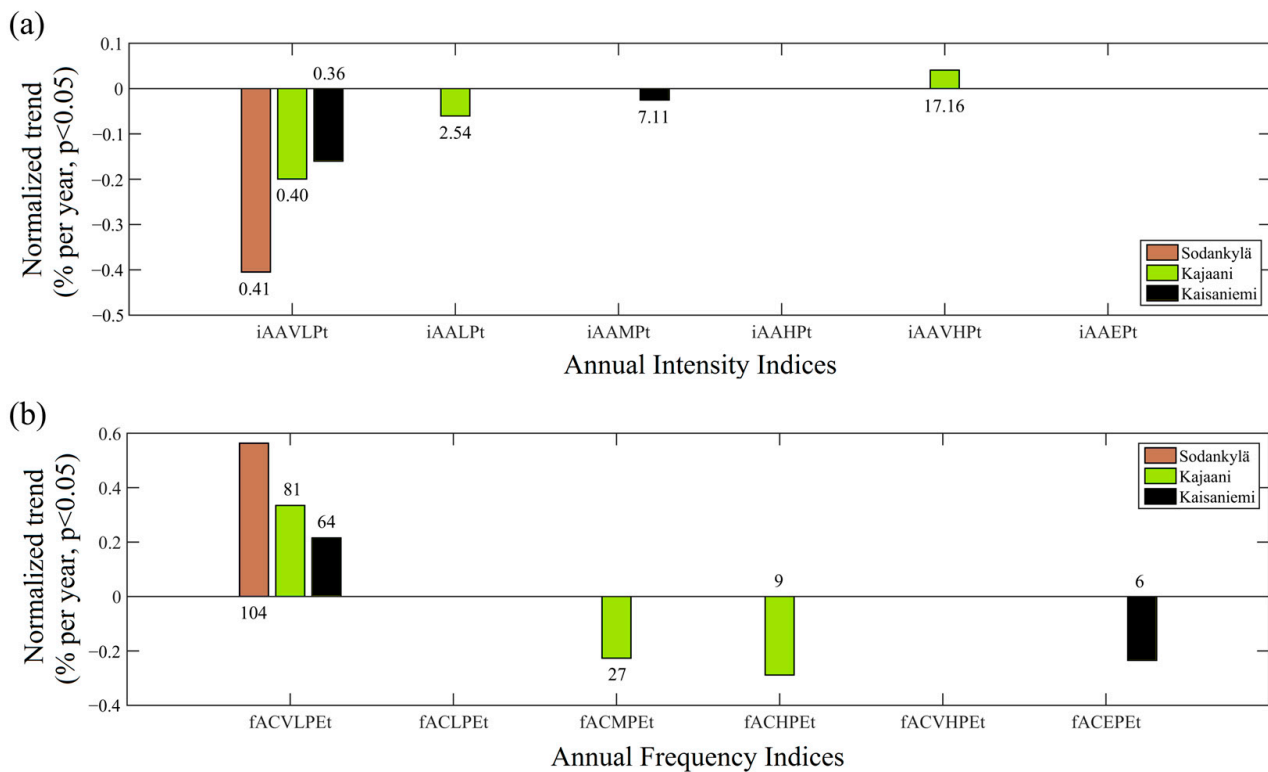


**Figure 3.** Normalized (% per year,  $p < 0.05$ ) inter-annual trends in daily precipitation (a) intensity and (b) frequency indices (Table 3) at the Sodankylä, Kajaani, and Kaisaniemi stations in northern, central, and southern Finland, respectively, during the period 1909–2023. The median values for normalized trends in annual indices at each studied station are presented on the top or bottom of the bars.

In general, both iAAVLp<sub>t</sub> and fACVLP<sub>t</sub> indices showed statistically significant ( $p < 0.05$ ) relationships with the SCAND pattern at Sodankylä (Figure 4) and Kajaani (Figure 5), while with the EA at Kaisaniemi (Figure 6). Both the intensity (iAALp<sub>t</sub>) and frequency (fACLp<sub>t</sub>) of light daily precipitation events were negatively associated with the NAO index at all three stations studied (Figures 4–6). However, the SCAND, EA/WR, and NAO were the influential climate teleconnections for variations in both iAAMP<sub>t</sub> and fACMP<sub>t</sub> indices at Sodankylä (Figure 4), Kajaani (Figure 5), and Kaisaniemi (Figure 6). For heavy daily precipitation events, both the intensity (iAAHP<sub>t</sub>) and frequency (fACHP<sub>t</sub>) were in significantly negative correlations with the EA/WR at Sodankylä (Figure 4), Kajaani (Figure 5), and Kaisaniemi (Figure 6). At all these stations, however, the very heavy daily precipitation intensity (iAAVHP<sub>t</sub>) and frequency (fACVHP<sub>t</sub>) indices showed positive relationships with the SCAND pattern (Figures 4–6). These teleconnections (the EA/WR and the SCAND) also controlled interannual variations in the intensity (iAAEP<sub>t</sub>) and frequency (fACEP<sub>t</sub>) of extreme daily precipitation at the Sodankylä (Figure 4), Kajaani (Figure 5), and Kaisaniemi (Figure 6) stations. Figures 4–6 comprehensively represent the correlations of interannual variations in daily graded precipitation indices with the annual and seasonal large-scale climate teleconnections at the Sodankylä, Kajaani, and Kaisaniemi stations, respectively.

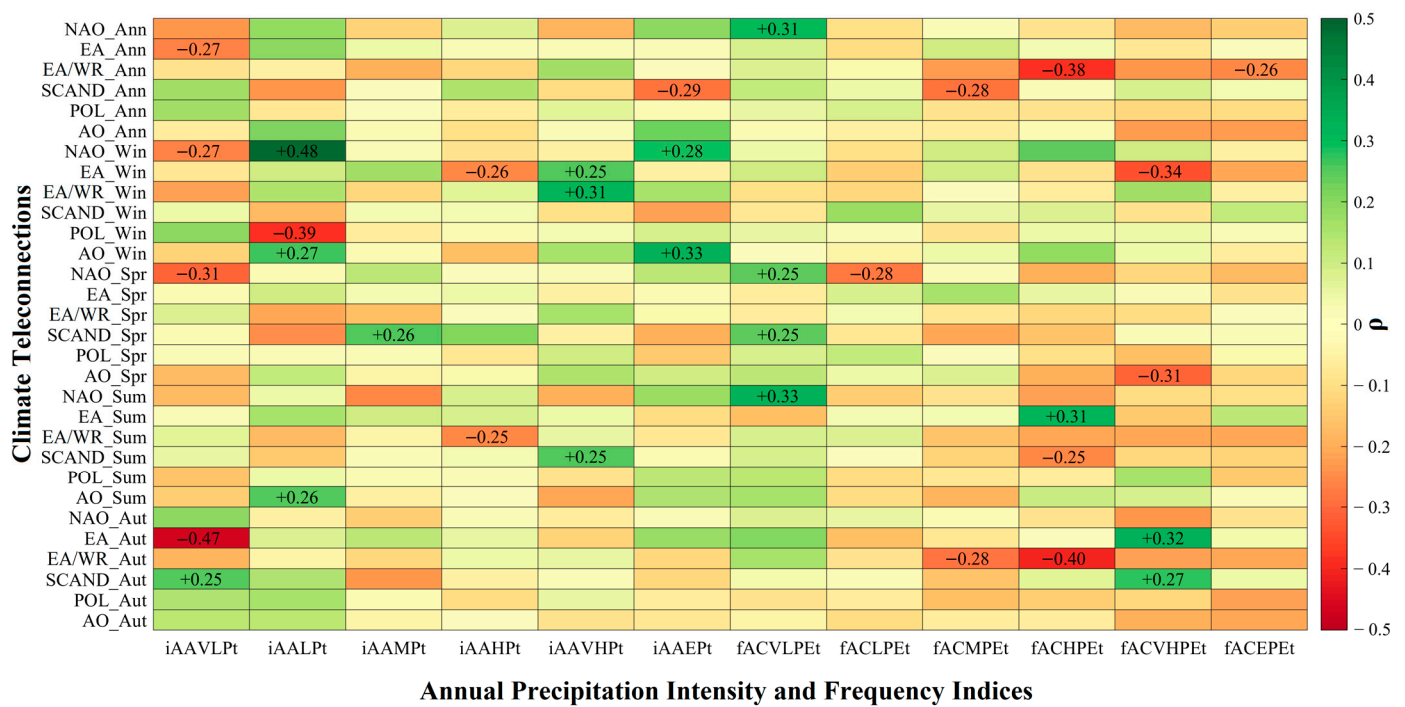


**Figure 4.** The Spearman’s rank correlations ( $\rho$ ) of annual precipitation intensity and frequency indices (Table 3) with the annual and seasonal climate teleconnections at the Sodankylä station in northern Finland during the period 1951–2023. The written values show statistically significant ( $p < 0.05$ ) correlations.

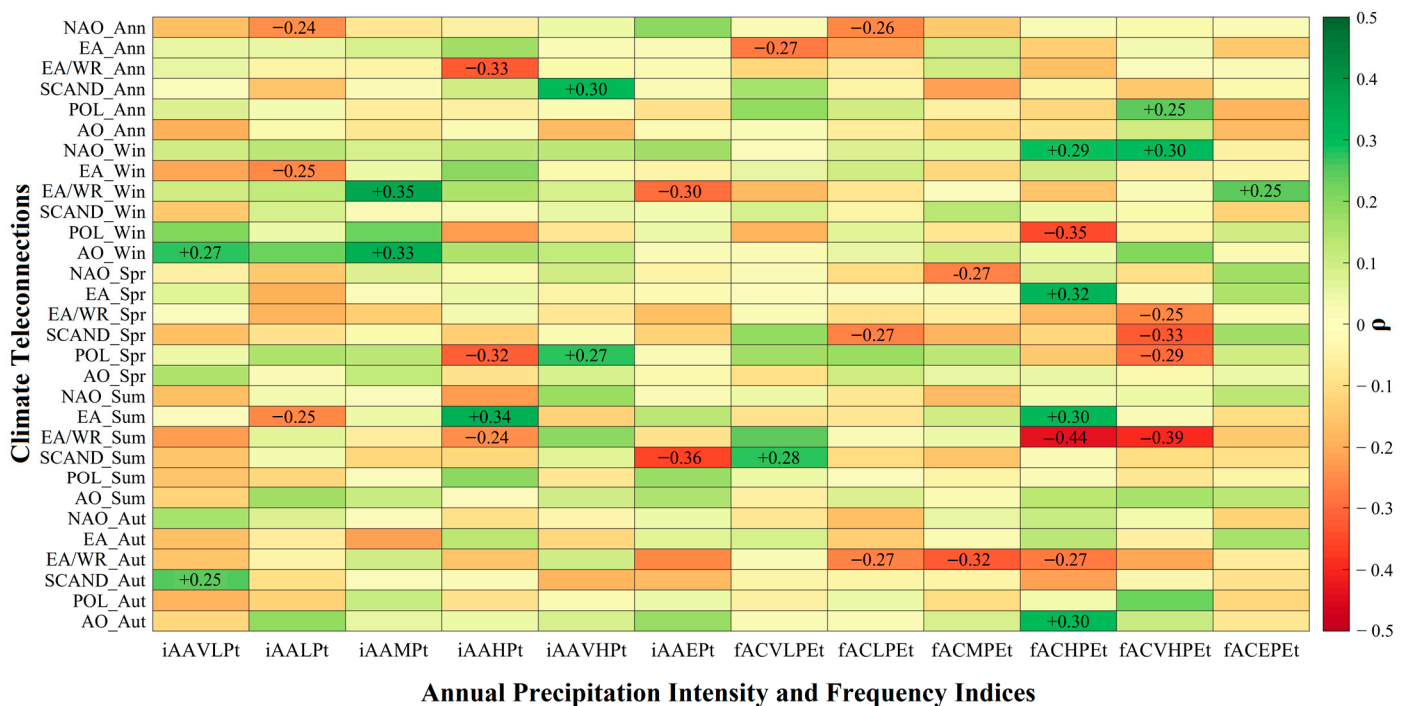


**Figure 5.** The Spearman’s rank correlations ( $\rho$ ) of annual precipitation intensity and frequency indices (Table 3) with the annual and seasonal climate teleconnections at the Kajaani station in central Finland during the period 1951–2023. The written values show statistically significant ( $p < 0.05$ ) correlations.



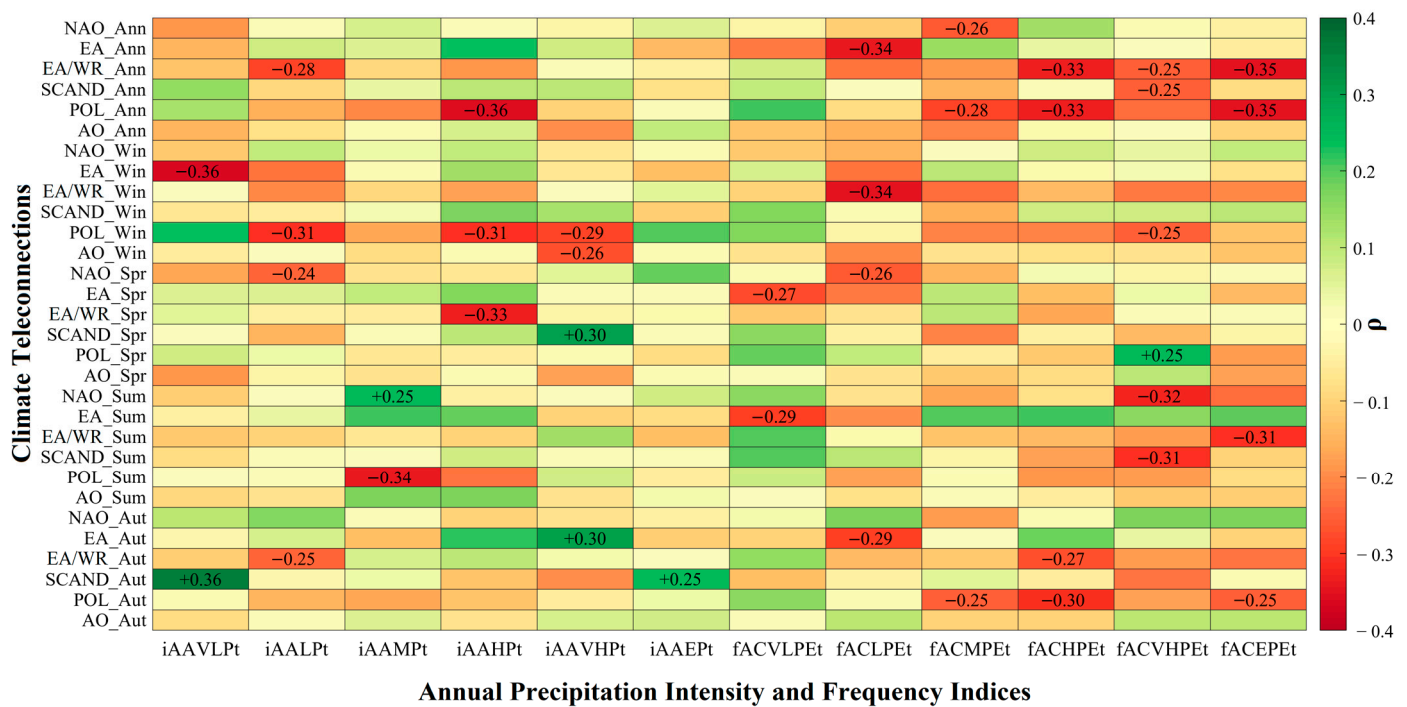


**Figure 6.** The Spearman’s rank correlations ( $\rho$ ) of annual precipitation intensity and frequency indices (Table 3) with the annual and seasonal climate teleconnections at the Kaisaniemi station in southern Finland during the period 1951–2023. The written values show statistically significant ( $p < 0.05$ ) correlations.

**4. Discussion**

*4.1. Variability and Trends in Graded Daily Precipitation Characteristics*

In Finland, daily precipitation intensity [42] and all extreme precipitation intensity indices [20] generally decrease from the northern to southern parts. The present study also found this spatial pattern in the intensity of graded daily precipitation events, except for both very light and moderate daily precipitation records that showed the highest amounts in central Finland. Such disagreement might be related to the different definitions used by these studies to calculate extreme daily precipitation intensities in Finland. In fact, applying percentiles by previous studies focusing on EPEs resulted in a similar spatial pattern to the mean precipitation variability across the country. Using different absolute daily precipitation amount boundaries, however, the present study improved our knowledge about which grades of daily precipitation intensity behave differently from the spatial distribution of precipitation values throughout Finland previously reported.

Defining the EPEs based on different percentile values, ref. [42] concluded that the extreme precipitation frequency increased from southern to northern Finland. However, ref. [20] determined that both relatively low and high extreme precipitation indices were more frequent in northern and southern Finland, respectively, during the period 1961–2011. The present study also indicated more frequencies of relatively low (high) EPEs in the north (south) than in the south (north) of Finland. As exceptions, we found the highest rates of frequency for both light and extreme daily precipitation grades at the Kajaani station in central Finland. Similarly, a few previous studies also reported such higher return values for relatively high EPEs in central Finland than in its other areas [62,63].

The present study detected statistically significant decreasing trends in the intensity of very light daily precipitation grades at all three hydrometeorological stations of Kaisaniemi, Kajaani, and Sodankyl in southern, central, and northern Finland, respectively, during the last 115 years (1909–2023). For the same stations, our previous study also reported such significant decreases in the very light amounts of daily precipitation calculated based on their 50th percentile values [42]. Both of these studies determined the highest rate of

such decreasing trends at the Sodankylä station in northern Finland. The lowest rates of such decreasing trends were found at Kaisaniemi in southern areas by our previous study [42] but at Kajaani in central parts by the present study. Similarly, [63] concluded substantial decreases in the moderate amounts of daily precipitation, defined based on their 60th percentile values, in Finland. Additionally, the present study found considerable decreasing (increasing) trends in light and moderate (very heavy) daily precipitation grades at Kajaani and Kaisaniemi (Kajaani) in central and southern (central) Finland, respectively, during the period 1909–2023. Such decreases, however, were not reported by previous studies. This might likely be related to the use of other hydrometeorological stations throughout Finland, the consideration of different study periods, and the application of dissimilar definitions for calculating EPEs. Like [42,63], moreover, the present study identified that heavy to extreme daily precipitation grades were mostly unchanged in Finland over time.

We found significant increasing trends in the frequency of very light precipitation grade in Finland during the period 1909–2023. The highest and lowest rates of these increases were seen in the north and south of this country, respectively. Such increasing trends and their spatial patterns throughout Finland were also reported previously by [42]. Despite such increases, the present study detected considerable decreasing trends in moderate and heavy (extreme) daily precipitation grades at Kajaani (Kaisaniemi) in central (southern) Finland over time. Less frequent moderate precipitation at Kajaani was similarly identified by our previous study [42]. When analyzing extreme precipitation indices, however, [20] showed no clear changes in the number of heavy (daily precipitation  $\geq 10$  mm) and very heavy (daily precipitation  $\geq 20$  mm) days, but it showed significant increases in wet days (daily precipitation  $\geq 1$  mm) in Finland during the period 1961–2011. At Kaisaniemi, Kajaani, and Sodankylä, no significant trends in heavy precipitation days were detected during the period 1910–1995 [64]. The other previous studies reported increases in very heavy precipitation frequency over Finland during the 20th century, particularly after 1980 [12,65]. The differences between our results and such previous studies are mainly because of the grading of daily precipitation records by the present study, which can provide us with more details about which amount boundaries of daily precipitation significantly contributed to changes in the frequency of EPEs greater than a certain threshold (e.g., 1 mm).

#### 4.2. Influential Climate Teleconnections

Across Finland, historical variations in annual precipitation were considerably associated with the SCAND and EA/WR patterns in 1911–2011 [39]. Statistically significant correlations between both the SCAND and EA/WR patterns and the ratio of annual total precipitation to the number of days with precipitation ( $>0$  mm) were also reported over Finland during the period 1908–2008 [42]. By analyzing extreme precipitation indices, similarly, ref. [20] concluded that the SCAND and EA/WR were the most influential climate teleconnections for interannual variability in total precipitation in wet days in Finland through the years 1961–2011. Likewise, the present study found substantial relationships between these two climate teleconnections—SCAND and EA/WR—and both the intensities and frequencies of moderate, heavy, very heavy, and extreme precipitation records, which are key components of annual precipitation in Finland. Additionally, this study discovered that the SCAND could also influence very light daily precipitation (between 0 and 1 mm) across the country, while the light daily precipitation (between 1 and 5 mm) was more evidently connected to the NAO during the period 1951–2023. This can be explained by the typical occurrence of very light (light) daily precipitation events during all months (cold months: December–May) of the year, for which the SCAND (NAO) generally influences precipitation variability across Finland [20,39]. Although our previous studies reported such relationships between climate teleconnections and EPEs in Finland, the present study improved our understating about the roles of the SCAND, EA/WR, and NAO in the spatio-

temporal variations in different daily precipitation grades as the primary contributors to the formation of EPEs across the country—an insight that has not yet been acknowledged.

The SCAND consists of a primary circulation center over the Scandinavian Peninsula and an extensive part of the Arctic Ocean throughout northern Siberia [48]. With the opposite sign of pressure anomalies, the two other action centers of this climate teleconnection (SCAND) are located over western Europe (the north-east Atlantic) and Mongolia (western China) [48]. The negative/positive phase of SCAND describes low/high pressure airflow inducing a colder/warmer and wetter/drier climate than normal conditions over Greenland, the Norwegian Sea, and the Scandinavian Peninsula [50]. This negative relationship was also evidenced by significant decreases in very light precipitation amounts in Finland, which were positively associated with the SCAND variability over time. However, considerable correlations between the SCAND and moderate, very heavy, and extreme daily precipitation events were not caused by any significant changes in their historical time series.

For Finland, the EA/WR describes the meridional circulation that naturally weakens when the westerly airflow strengthens. As a zonally oriented climate teleconnection, the EA/WR principally consists of two action centers over western Europe and the Caspian Sea in winter, while the other three pressure anomaly centers are in the coastal areas of Portugal, northwestern Europe, and the western–northwestern parts of Russia during both spring and autumn seasons [48]. The negative/positive phase of this climate teleconnection (EA/WR) is fundamentally associated with the southeasterly/northwesterly and southerly/northerly airflows over the Baltic Sea and the East European Plain [49]. Accordingly, the positive phase of EA/WR principally brings a warmer and wetter (colder and drier) climate than normal conditions across East Asia (the Arctic area, large parts of western Russia, and northeast Africa) [49]. This study confirmed such relationships by measuring significant negative correlations between increasing EA/WR values [66] and heavy daily precipitation events, resulting in their lower frequency at the Kajaani station located close to western Russia in recent decades.

Besides such effects of SCAND (EA/WR) on very light, moderate, very heavy, and extreme (heavy) daily precipitation, this study also determined the substantial negative correlations of NAO with both the intensity and frequency of light daily precipitation records in Finland. This climate teleconnection (NAO) is a numeric index for describing the power of westerlies from the North Atlantic to the Atlantic parts of Europe [47]. Hence, the positive/negative NAO phase generally corresponds to the strengthening and weakening of westerly airflows, bringing a milder and wetter/colder and drier climate than normal conditions over the north of Europe, particularly during the cold months (Dec–May) [67,68]. Based on [69], the NAO power increased by 0.20 decade<sup>-1</sup> in recent decades. Despite significant negative relationships between this climate teleconnection (NAO) and light daily precipitation events, such an increasing trend in the NAO caused no clear changes in the intensity and frequency of this daily precipitation grade (light) across Finland. As the only exception, however, the Kajaani station in central Finland experienced a significant decreasing trend in the intensity of light daily precipitation over time.

## 5. Conclusions

This study analyzed variability and trends in daily graded (from very light to extreme) precipitation records at three hydrometeorological stations of Kaisaniemi, Kajaani, and Sodankylä in southern, central, and northern Finland during the last 115 years (1909–2023). The relationships of such variability and trends with large-scale, well-known climate teleconnections were also measured for the period of 1951–2023. The major conclusions were:

- In general, more intense but less frequent very light daily precipitation events were recorded in Finland during the period 1909–2023. The Sodankylä (Kaisaniemi) station in northern (southern) Finland experienced the highest (lowest) rates of such decreases and increases in the intensity and frequency of historical very light precipitation events. At Kajaani in central Finland, however, the intensities of light daily precipitation events

showed a significant decreasing trend during the period 1909–2023. At this station, statistically significant trends were also detected in both the intensity and frequency of heavy daily precipitation events over time.

- The SCAND (EA) pattern was the strongest climate teleconnection positively (negatively) influencing the variability in both the intensity and frequency of very light daily events in northern and central (southern) Finland during the period 1951–2023. At all three stations of Sodankylä, Kajaani, and Kaisaniemi, however, both the intensity and frequency of light daily precipitation events showed substantial negative relationships with the NAO in the last 70 years. The SCAND and NAO also influenced the variations in both the intensity and frequency of historical moderate daily precipitation events at all three stations studied. The intensities and frequencies of all heavy (very heavy and extreme) daily precipitation events in Finland, however, were mainly controlled by variations in the EA/WR (SCAND) pattern over time. Hence, the SCAND was the most influential climate teleconnection for variations in both the intensities and frequencies of all daily graded precipitation events in Finland, except for light daily precipitation records significantly associated with the NAO over time.

Such conclusions can lay the foundation for developing adaptation and mitigation strategies for sustainable water resources management in the boreal environment of Finland and supporting this country in achieving economic, social, and environmental sustainability under global warming and climate change.

**Author Contributions:** Conceptualization, M.I. and Z.A.; methodology, M.I., Z.A. and R.A.; software, R.A. and F.A.; validation, F.A. and G.S.; formal analysis, M.I., G.S. and H.A.; investigation, M.I., Z.A. and H.A.; resources, M.I.; data curation, Z.A. and R.A.; writing—original draft preparation, M.I., Z.A. and R.A.; writing—review and editing, M.I.; visualization, M.I., Z.A. and F.A.; supervision, M.I.; project administration, M.I.; funding acquisition, M.I. All authors have read and agreed to the published version of the manuscript.

**Funding:** This study was funded by the Sakari Alhopuro Foundation (Grant Nos. 20220247 and 20230218) and the Maa- ja vesi tekniikan tuki r.y. (Grant Nos. 44008 and 45599).

**Data Availability Statement:** All datasets analyzed during this study are publicly available through the references given in the manuscript.

**Acknowledgments:** We would like to acknowledge the Finnish Meteorological Institute (FMI) for recording historical daily SAT and precipitation in Finland and the Finnish Environment Institute (SYKE) at the hydrometeorological measurement stations studied. We are also grateful to the Climate Prediction Center (CPC) at the National Oceanic and Atmospheric Administration (NOAA) of the United States for making available online the standardized monthly values of climate teleconnections used in this study.

**Conflicts of Interest:** The authors declare that they have no known competing financial interests or personal relationships that could have appeared to influence the work reported in this paper.

## References

1. IPCC; Masson-Delmotte, V.; Zhai, P.; Pirani, A.; Connors, S.L.; Péan, C.; Berger, S.; Caud, N.; Chen, Y.; Goldfarb, L.; et al. *Climate Change 2021: The Physical Science Basis. Contribution of Working Group I to the Sixth Assessment Report of the Intergovernmental Panel on Climate Change*; Intergovernmental Panel on Climate Change: Geneva, Switzerland, 2021.
2. Iz, H.B. Is the Global Sea Surface Temperature Rise Accelerating? *Geod. Geodyn.* **2018**, *9*, 432–438. [[CrossRef](#)]
3. Ali, H.; Mishra, V. Contrasting Response of Rainfall Extremes to Increase in Surface Air and Dewpoint Temperatures at Urban Locations in India. *Sci. Rep.* **2017**, *7*, 1228. [[CrossRef](#)] [[PubMed](#)]
4. Kirchmeier-Young, M.C.; Zhang, X. Human Influence Has Intensified Extreme Precipitation in North America. *Proc. Natl. Acad. Sci. USA* **2020**, *117*, 13308–13313. [[CrossRef](#)] [[PubMed](#)]
5. Tabari, H.; Madani, K.; Willems, P. The Contribution of Anthropogenic Influence to More Anomalous Extreme Precipitation in Europe. *Environ. Res. Lett.* **2020**, *15*, 104077. [[CrossRef](#)]
6. Irannezhad, M.; Liu, J.; Chen, D. Extreme Precipitation Variability across the Lancang-Mekong River Basin during 1952–2015 in Relation to Teleconnections and Summer Monsoons. *Int. J. Climatol.* **2022**, *42*, 2614–2638. [[CrossRef](#)]
7. Liu, A.; Soneja, S.I.; Jiang, C.; Huang, C.; Kerns, T.; Beck, K.; Mitchell, C.; Sapkota, A. Frequency of Extreme Weather Events and Increased Risk of Motor Vehicle Collision in Maryland. *Sci. Total Environ.* **2017**, *580*, 550–555. [[CrossRef](#)]

8. Ohba, M.; Sugimoto, S. Differences in Climate Change Impacts between Weather Patterns: Possible Effects on Spatial Heterogeneous Changes in Future Extreme Rainfall. *Clim. Dyn.* **2019**, *52*, 4177–4191. [[CrossRef](#)]
9. Rummukainen, M. Changes in Climate and Weather Extremes in the 21st Century. *WIREs Clim. Chang.* **2012**, *3*, 115–129. [[CrossRef](#)]
10. Donat, M.G.; Alexander, L.V.; Yang, H.; Durre, I.; Vose, R.; Dunn, R.J.H.; Willett, K.M.; Aguilar, E.; Brunet, M.; Caesar, J.; et al. Updated Analyses of Temperature and Precipitation Extreme Indices since the Beginning of the Twentieth Century: The HadEX2 Dataset. *J. Geophys. Res. Atmos.* **2013**, *118*, 2098–2118. [[CrossRef](#)]
11. Liu, B.; Tan, X.; Gan, T.Y.; Chen, X.; Lin, K.; Lu, M.; Liu, Z. Global Atmospheric Moisture Transport Associated with Precipitation Extremes: Mechanisms and Climate Change Impacts. *WIREs Water* **2020**, *7*, e1412. [[CrossRef](#)]
12. Alexander, L.V.; Zhang, X.; Peterson, T.C.; Caesar, J.; Gleason, B.; Klein Tank, A.M.G.; Haylock, M.; Collins, D.; Trewin, B.; Rahimzadeh, F.; et al. Global Observed Changes in Daily Climate Extremes of Temperature and Precipitation. *J. Geophys. Res. Atmos.* **2006**, *111*, D05109. [[CrossRef](#)]
13. Zhang, X.; Alexander, L.; Hegerl, G.C.; Jones, P.; Tank, A.K.; Peterson, T.C.; Trewin, B.; Zwiers, F.W. Indices for Monitoring Changes in Extremes Based on Daily Temperature and Precipitation Data. *WIREs Clim. Chang.* **2011**, *2*, 851–870. [[CrossRef](#)]
14. Serinaldi, F.; Kilsby, C.G. Stationarity Is Undead: Uncertainty Dominates the Distribution of Extremes. *Adv. Water Resour.* **2015**, *77*, 17–36. [[CrossRef](#)]
15. Kim, H.; Kim, S.; Shin, H.; Heo, J.-H. Appropriate Model Selection Methods for Nonstationary Generalized Extreme Value Models. *J. Hydrol.* **2017**, *547*, 557–574. [[CrossRef](#)]
16. Liu, S.; Huang, S.; Huang, Q.; Xie, Y.; Leng, G.; Luan, J.; Song, X.; Wei, X.; Li, X. Identification of the Non-Stationarity of Extreme Precipitation Events and Correlations with Large-Scale Ocean-Atmospheric Circulation Patterns: A Case Study in the Wei River Basin, China. *J. Hydrol.* **2017**, *548*, 184–195. [[CrossRef](#)]
17. Fu, J.; Qian, W.; Lin, X.; Chen, D. Trends in Graded Precipitation in China from 1961 to 2000. *Adv. Atmos. Sci.* **2008**, *25*, 267–278. [[CrossRef](#)]
18. Hu, M.; Dong, M.; Tian, X.; Wang, L.; Jiang, Y. Trends in Different Grades of Precipitation over the Yangtze River Basin from 1960 to 2017. *Atmosphere* **2021**, *12*, 413. [[CrossRef](#)]
19. Xie, M.; Ren, Z.; Li, Z.; Zhang, X.; Ma, X.; Li, P.; Shen, Z. Evolution of the Precipitation–Stream Runoff Relationship in Different Precipitation Scenarios in the Yellow River Basin. *Urban Clim.* **2023**, *51*, 101609. [[CrossRef](#)]
20. Irannezhad, M.; Chen, D.; Kløve, B.; Moradkhani, H. Analysing the Variability and Trends of Precipitation Extremes in Finland and Their Connection to Atmospheric Circulation Patterns. *Int. J. Climatol.* **2017**, *37*, 1053–1066. [[CrossRef](#)]
21. Pedretti, D.; Irannezhad, M. Non-Stationary Peaks-over-Threshold Analysis of Extreme Precipitation Events in Finland, 1961–2016. *Int. J. Climatol.* **2019**, *39*, 1128–1143. [[CrossRef](#)]
22. Liu, Y.; Zhang, C.; Tang, Q.; Hosseini-Moghari, S.-M.; Haile, G.G.; Li, L.; Li, W.; Yang, K.; van der Ent, R.J.; Chen, D. Moisture Source Variations for Summer Rainfall in Different Intensity Classes over Huaihe River Valley, China. *Clim. Dyn.* **2021**, *57*, 1121–1133. [[CrossRef](#)]
23. Pathak, A.; Ghosh, S.; Martinez, J.A.; Dominguez, F.; Kumar, P. Role of Oceanic and Land Moisture Sources and Transport in the Seasonal and Interannual Variability of Summer Monsoon in India. *J. Clim.* **2017**, *30*, 1839–1859. [[CrossRef](#)]
24. Jiang, Z.; Jiang, S.; Shi, Y.; Liu, Z.; Li, W.; Li, L. Impact of Moisture Source Variation on Decadal-Scale Changes of Precipitation in North China from 1951 to 2010. *J. Geophys. Res. Atmos.* **2017**, *122*, 600–613. [[CrossRef](#)]
25. Zhu, Y.; Sang, Y.-F.; Chen, D.; Sivakumar, B.; Li, D. Effects of the South Asian Summer Monsoon Anomaly on Interannual Variations in Precipitation over the South-Central Tibetan Plateau. *Environ. Res. Lett.* **2020**, *15*, 124067. [[CrossRef](#)]
26. Chen, D.; Chen, Y. Association between Winter Temperature in China and Upper Air Circulation over East Asia Revealed by Canonical Correlation Analysis. *Glob. Planet. Change* **2003**, *37*, 315–325. [[CrossRef](#)]
27. Glantz, M.H.; Katz, R.; Nicholls, N. (Eds.) *Teleconnections Linking Worldwide Climate Anomalies: Scientific Basis and Societal Impact*; Cambridge University Press: Cambridge, UK, 2009; ISBN 9780521106849, 0521106842.
28. Wang, B.; Lee, M.-Y.; Xie, Z.; Lu, M.; Pan, M. A New Asian/North American Teleconnection Linking Clustered Extreme Precipitation from Indian to Canada. *NPJ Clim. Atmos. Sci.* **2022**, *5*, 90. [[CrossRef](#)]
29. Zhang, X.; Chen, Y.; Fang, G.; Li, Y.; Li, Z.; Wang, F.; Xia, Z. Observed Changes in Extreme Precipitation over the Tianshan Mountains and Associated Large-Scale Climate Teleconnections. *J. Hydrol.* **2022**, *606*, 127457. [[CrossRef](#)]
30. Kang, X.; Min, R.; Dai, J.; Gu, X. The Role of Teleconnection in the Occurrence Probability of Extreme Precipitation over China Based on Extreme Value Theory. *Front. Environ. Sci.* **2022**, *10*, 1013636. [[CrossRef](#)]
31. Biswas, J. Unravelling the Influence of Teleconnection Patterns on Monsoon Extreme Precipitation Indices over the Sikkim Himalayas and West Bengal. *J. Hydrol.* **2023**, *618*, 129148. [[CrossRef](#)]
32. Ghasemifar, E.; Irannezhad, M.; Minaei, F.; Minaei, M. The Role of ENSO in Atmospheric Water Vapor Variability during Cold Months over Iran. *Theor. Appl. Climatol.* **2022**, *148*, 795–817. [[CrossRef](#)]
33. Irannezhad, M.; Ahmadi, B.; Liu, J.; Chen, D.; Matthews, J.H. Global Water Security: A Shining Star in the Dark Sky of Achieving the Sustainable Development Goals. *Sustain. Horiz.* **2022**, *1*, 100005. [[CrossRef](#)]
34. Nations, United. *About the Sustainable Development Goals—United Nations Sustainable Development*; United Nations Development Programme: New York, NY, USA, 2015.

35. Chen, D.; Chen, H.W. Using the Köppen Classification to Quantify Climate Variation and Change: An Example for 1901–2010. *Environ. Dev.* **2013**, *6*, 69–79. [[CrossRef](#)]
36. Käyhkö, J. Muuttuuko Pohjolan Ilmasto? (Fennoscandian Climate in Change?). *Publ. Geogr. Dep. Univ. Turku* **2004**, *168*, 19–35.
37. Peel, M.C.; Finlayson, B.L.; McMahon, T.A. Updated World Map of the Köppen–Geiger Climate Classification. *Hydrol. Earth Syst. Sci.* **2007**, *11*, 1633–1644. [[CrossRef](#)]
38. Irannezhad, M.; Chen, D.; Kløve, B. Interannual Variations and Trends in Surface Air Temperature in Finland in Relation to Atmospheric Circulation Patterns, 1961–2011. *Int. J. Climatol.* **2015**, *35*, 3078–3092. [[CrossRef](#)]
39. Irannezhad, M.; Marttila, H.; Kløve, B. Long-Term Variations and Trends in Precipitation in Finland. *Int. J. Climatol.* **2014**, *34*, 3139–3153. [[CrossRef](#)]
40. Jokinen, P.; Kaukoranta, J.-P.; Kangas, A.; Alenius, P.; Eriksson, P.; Johansson, M.; Wilkman, S. *Tilastoja Suomen Ilmastosta ja Merestä 1991–2020*; Finnish Meteorological Institute: Helsinki, Finland, 2021.
41. Irannezhad, M.; Ronkanen, A.K.; Kløve, B. Effects of Climate Variability and Change on Snowpack Hydrological Processes in Finland. *Cold Reg. Sci. Technol.* **2015**, *118*, 14–29. [[CrossRef](#)]
42. Irannezhad, M.; Marttila, H.; Chen, D.; Kløve, B. Century-Long Variability and Trends in Daily Precipitation Characteristics at Three Finnish Stations. *Adv. Clim. Chang. Res.* **2016**, *7*, 54–69. [[CrossRef](#)]
43. Irannezhad, M.; Ronkanen, A.-K.; Kløve, B. Wintertime Climate Factors Controlling Snow Resource Decline in Finland. *Int. J. Climatol.* **2016**, *36*, 110–131. [[CrossRef](#)]
44. Solantie, R.; Junila, P. *Sademäärien Korjaaminen Tretjakovin Ja Wildin Sademittarien Vertailumittausten Avulla, Summary in English: The Correction of Precipitation Measurements Based on Comparisons between Tretjakov and Wild Gauges*; Finnish Meteorological Institute: Helsinki, Finland, 1995.
45. Irannezhad, M.; Torabi Haghghi, A.; Chen, D.; Kløve, B. Variability in Dryness and Wetness in Central Finland and the Role of Teleconnection Patterns. *Theor. Appl. Climatol.* **2015**, *122*, 471–486. [[CrossRef](#)]
46. Irannezhad, M.; Chen, D.; Kløve, B. The Role of Atmospheric Circulation Patterns in Agroclimate Variability in Finland, 1961–2011. *Geogr. Ann. Ser. A, Phys. Geogr.* **2016**, *98*, 287–301. [[CrossRef](#)]
47. Thompson, D.W.J.; Wallace, J.M. The Arctic Oscillation Signature in the Wintertime Geopotential Height and Temperature Fields. *Geophys. Res. Lett.* **1998**, *25*, 1297–1300. [[CrossRef](#)]
48. Barnston, A.G.; Livezey, R.E. Classification, Seasonality and Persistence of Low-Frequency Atmospheric Circulation Patterns. *Mon. Weather Rev.* **1987**, *115*, 1083–1126. [[CrossRef](#)]
49. Lim, Y.K.; Kim, H.D. Impact of the Dominant Large-Scale Teleconnections on Winter Temperature Variability over East Asia. *J. Geophys. Res. Atmos.* **2013**, *118*, 7835–7848. [[CrossRef](#)]
50. Bueh, C.; Nakamura, H. Scandinavian Pattern and Its Climatic Impact. *Q. J. R. Meteorol. Soc.* **2007**, *133*, 2117–2131. [[CrossRef](#)]
51. Mann, H.B. Non-Parametric Test Against Trend. *Econometrica* **1945**, *13*, 245–259. [[CrossRef](#)]
52. Kendall, M.G. *Rank Correlation Methods*; Oxford University Press: Oxford, UK, 1948.
53. Yue, S.; Pilon, P.; Phinney, B.; Cavadias, G. The Influence of Autocorrelation on the Ability to Detect Trend in Hydrological Series. *Hydrol. Process.* **2002**, *16*, 1807–1829. [[CrossRef](#)]
54. Sen, P.K. Estimates of the Regression Coefficient Based on Kendall’s Tau. *J. Am. Stat. Assoc.* **1968**, *63*, 1379–1389. [[CrossRef](#)]
55. Helsel, D.R.; Hirsch, R.M. *Statistical Methods in Water Resources*; U.S. Geological Survey: Reston, VA, USA, 1992.
56. Park, E.; Lee, Y.J. Estimates of Standard Deviation of Spearman’s Rank Correlation Coefficients with Dependent Observations. *Commun. Stat. Part B Simul. Comput.* **2001**, *30*, 129–142. [[CrossRef](#)]
57. Irannezhad, M.; Kløve, B. Do Atmospheric Teleconnection Patterns Explain Variations and Trends in Thermal Growing Season Parameters in Finland? *Int. J. Climatol.* **2015**, *35*, 4619–4630. [[CrossRef](#)]
58. Kiani, S.; Irannezhad, M.; Ronkanen, A.-K.; Moradkhani, H.; Kløve, B. Effects of Recent Temperature Variability and Warming on the Oulu–Hailuoto Ice Road Season in the Northern Baltic Sea. *Cold Reg. Sci. Technol.* **2018**, *151*, 1–8. [[CrossRef](#)]
59. Irannezhad, M.; Liu, J.; Chen, D. Influential Climate Teleconnections for Spatiotemporal Precipitation Variability in the Lancang–Mekong River Basin from 1952 to 2015. *J. Geophys. Res. Atmos.* **2020**, *125*, e2020JD033331. [[CrossRef](#)]
60. Irannezhad, M.; Abdullah Abdulghafour, Z.; Marttila, H. Annual and Seasonal Mean Daily Discharge in Natural and Regulated Rivers in Northern Finland: Variability, Trends, and Links to Climate Teleconnections. *Hydrol. Res.* **2024**, nh2024041. [[CrossRef](#)]
61. Irannezhad, M.; Abdulghafour, Z.; Sadeqi, A. Climate Teleconnections Influencing Historical Variations, Trends, and Shifts in Snow Cover Days in Finland. In *Earth Systems and Environment*; Springer: Berlin/Heidelberg, Germany, 2024. [[CrossRef](#)]
62. Venäläinen, A.; Jylhä, K.; Kilpeläinen, T.; Saku, S.; Tuomenvirta, H.; Vajda, A.; Ruosteenoja, K. Recurrence of Heavy Precipitation, Dry Spells and Deep Snow Cover in Finland Based on Observations. *Boreal Environ. Res.* **2009**, *14*, 166–172.
63. Wen, G.; Huang, G.; Hu, K.; Qu, X.; Tao, W.; Gong, H. Changes in the Characteristics of Precipitation over Northern Eurasia. *Theor. Appl. Climatol.* **2015**, *119*, 653–665. [[CrossRef](#)]
64. Heino, R.; Brázdil, R.; Førland, E.; Tuomenvirta, H.; Alexandersson, H.; Beniston, M.; Pfister, C.; Rebetz, M.; Rosenhagen, G.; Rösner, S.; et al. Progress in the Study of Climatic Extremes in Northern and Central Europe. *Clim. Change* **1999**, *42*, 151–181. [[CrossRef](#)]
65. Groisman, P.Y.; Knight, R.W.; Easterling, D.R.; Karl, T.R.; Hegerl, G.C.; Razuvaev, V.N. Trends in Intense Precipitation in the Climate Record. *J. Clim.* **2005**, *18*, 1326–1350. [[CrossRef](#)]

66. Krichak, S.O.; Kishcha, P.; Alpert, P. Decadal Trends of Main Eurasian Oscillations and the Eastern Mediterranean Precipitation. *Theor. Appl. Climatol.* **2002**, *72*, 209–220. [[CrossRef](#)]
67. Gormsen, A.K.; Hense, A.; Toldam-Andersen, T.B.; Braun, P. Large-Scale Climate Variability and Its Effects on Mean Temperature and Flowering Time of Prunus and Betula in Denmark. *Theor. Appl. Climatol.* **2005**, *82*, 41–50. [[CrossRef](#)]
68. Jaagus, J. Climatic Changes in Estonia during the Second Half of the 20th Century in Relationship with Changes in Large-Scale Atmospheric Circulation. *Theor. Appl. Climatol.* **2006**, *83*, 77–88. [[CrossRef](#)]
69. Wang, D.; Wang, C.; Yang, X.; Lu, J. Winter Northern Hemisphere Surface Air Temperature Variability Associated with the Arctic Oscillation and North Atlantic Oscillation. *Geophys. Res. Lett.* **2005**, *32*, L16706.1–L16706.4. [[CrossRef](#)]

**Disclaimer/Publisher’s Note:** The statements, opinions and data contained in all publications are solely those of the individual author(s) and contributor(s) and not of MDPI and/or the editor(s). MDPI and/or the editor(s) disclaim responsibility for any injury to people or property resulting from any ideas, methods, instructions or products referred to in the content.